

Application of the Disk Evaporation Model to AGNs

B. F. Liu¹

bfliu@ynao.ac.cn

and

Ronald E. Taam^{2,3,4}

r-taam@northwestern.edu

ABSTRACT

The disk corona evaporation model extensively developed for the interpretation of observational features of black hole X-ray binaries (BHXRBS) is applied to AGNs. Since the evaporation of gas in the disk can lead to its truncation for accretion rates less than a maximal evaporation rate, the model can naturally account for the soft spectrum in high luminosity AGNs and the hard spectrum in low luminosity AGNs. The existence of two different luminosity levels describing transitions from the soft to hard state and from the hard to soft state in BHXRBS, when applied to AGNs, suggests that AGNs can be in either spectral state within a range of luminosities. For example, at a viscosity parameter, α , equal to 0.3, the Eddington ratio from the hard to soft transition and from the soft to hard transition occurs at 0.027 and 0.005 respectively. The differing Eddington ratios result from the importance of Compton cooling in the latter transition, in which the cooling associated with soft photons emitted by the optically thick inner disk in the soft spectral state inhibits evaporation. When the Eddington ratio of the AGN lies below the critical value corresponding to its evolutionary state, the disk is truncated. With decreasing Eddington ratios, the inner edge of the disk increases to greater distances from the black hole with a concomitant increase

¹National Astronomical Observatories/Yunnan Observatory, Chinese Academy of Sciences, P.O. Box 110, Kunming 650011, China

²Academia Sinica Institute of Astrophysics and Astronomy-TIARA, P.O. Box 23-141, Taipei, 10617 Taiwan

³Academia Sinica Institute of Astrophysics and Astronomy/National Tsing Hua University-TIARA, Hsinchu Taiwan

⁴Northwestern University, Department of Physics and Astronomy, 2131 Tech Drive, Evanston, IL 60208

in the inner radius of the broad line region, R_{BLR} . The absence of an optically thick inner disk at low luminosities (L) gives rise to region in the $R_{BLR} - L$ plane for which the relation $R_{BLR} \propto L^{1/2}$ inferred at high luminosities is excluded. As a result, a lower limit to the accretion rate is predicted for the observability of broad emission lines, if the broad line region is associated with an optically thick accretion disk. Thus, true Seyfert 2 galaxies may exist at very low accretion rates/luminosities. The differences between BHXRBS and AGNs in the framework of the disk corona model are discussed and possible modifications to the model are briefly suggested.

Subject headings: accretion, accretion disks — black hole physics —galaxies: active — X-rays:galaxies

1. Introduction

The structure of accretion disks surrounding compact objects is central to our understanding of both stellar mass black holes in X-ray binary systems and supermassive black holes in the nuclei of galaxies. Among the issues requiring elucidation is the physical description of the accretion flow in the sources' spectral states. Toward this end, Shakura & Sunyaev (1973) pioneered the development of optically thick and geometrically thin accretion disks within the framework of a turbulent α disk model, which provided an explanation of the thermal state of these sources. Recognizing the possibility of physically distinct states in the disk to explain the hard X-ray state of Cyg X-1 (e.g., Agrawal et al. 1972; Tananbaum et al. 1972), Shapiro, Lightman, & Eardley (1976) and Ichimaru (1977) proposed a geometrically thick and optically thin accretion flow model. More recently, Narayan & Yi (1994, 1995a, 1995b) and Abramowicz et al. (1995) have stressed the importance of the advection of accretion energy stored in the accreting gas, leading to radiative inefficient accretion in the so-called advection-dominated accretion flow (ADAF). The investigation of the features of these ADAF models and their application to the spectral states of black hole X-ray binary systems and AGNs has been discussed in the reviews of Narayan, Mahadevan, & Quataert (1998), Narayan (2005), and Narayan & McClintock (2008).

The high/soft state spectrum of BHXRBS is generally believed to originate from an accretion disk extending to the innermost stable circular orbit (ISCO) as developed by Shakura & Sunyaev (1973), whereas the low/hard state spectrum is thought to originate in a geometrically thick, optically thin, hot corona or ADAF in the immediate vicinity of the black hole (see Narayan & Yi 1994; 1995a, b). We note that the observational data of accreting black holes commonly point to the coexistence of hot and cool accretion flows, which is likely to

be either in the form of an inner ADAF connecting to an outer geometrically thin disk or an ADAF-like corona lying above a standard thin disk extending to the ISCO. The former configuration has been studied by Esin et al. (1997) and applied to both quiescent BHXRBS and low-luminosity AGNs. In contrast, the latter configuration was proposed to explain the power-law X-ray emission and lower-frequency blackbody component observed in both BHXRBS and AGNs (e.g., see Liang & Price 1977; Haardt & Maraschi 1991; Nakamura & Osaki 1993). In the context of these studies, only the disk evaporation model (e.g. Meyer et al. 2000a) has been investigated in detail to elucidate the nature of the interaction between the disk and the corona.

Such an evaporation model has been reasonably successful in providing an interpretive framework of the many features observed in BHXRBS. For example, the spectral transition between the low/hard and high/soft state (Meyer et al. 2000b), the disk truncation and formation of an ADAF in the low/hard state (Liu et al. 1999; Meyer-Hofmeister & Meyer 2003), the luminosity hysteresis between the hard-to-soft and soft-to-hard transitions (Meyer-Hofmeister et al. 2005; Liu et al. 2005), the intermediate state (Liu et al. 2006; Meyer et al. 2007), and the inner cool disk component in the low/hard state (Liu et al. 2007; Taam et al. 2008) can all be understood as consequences of the disk evaporation/condensation process. The model provides a physical basis for understanding the observational phenomenology, although details remain to be addressed.

As is well known, observations of AGNs exhibit many similar features to BHXRBS. Of importance is the existence of the fundamental plane (Merloni et al. 2003; Falcke et al. 2004; Wang et al. 2006) relating the radio luminosity, X-ray luminosity and black hole mass which extends from stellar masses to supermassive black holes. In addition to these relations, the differing spectral shapes between high luminosity AGNs (HLAGNs) and low luminosity AGNs (LLAGNs) (e.g., Elvis et al. 1994; Ho 1999; Ho 2008 and reference therein) are widely observed. Specifically, the HLAGNs, such as quasars and some Seyfert galaxies, display evidence of disk accretion as inferred from the presence of a “big blue bump” and hence are the analogues of high/soft state BHXRBS (Maccarone et al. 2003). On the other hand, LLAGNs exhibit hard X-ray emission as illustrated, for example, by our Galactic Center (Narayan & Yi 1994; Yuan et al. 2003; Narayan 2005) and/or evidence of radio jets and are analogues of the low/hard state BHXRBS (for a review see Ho 2008). Spectral features seen in narrow line Seyfert 1 galaxies (NLS1) are similar to BHXRBS at the very high states (e.g. Pounds et al. 1995; Pounds & Vaughan 2000). Although there exist differences (e.g., a soft X-ray excess is often seen in AGNs), a phenomenology based on a unification scheme for the BHXRBS and AGNs has been proposed (Falcke et al. 2004; Fender et al. 2004; Ho 2009).

In these models, the transition from an outer disk to an inner ADAF is one of the primary issues remaining to be clarified. Among the mechanisms facilitating the state transition (see Honma 1996; Manmoto & Kato 2000; Meyer et al. 2000b; Różańska & Czerny 2000a,b; Spruit & Deufel 2002; Lu et al. 2004; Dullemond & Spruit 2005), the disk corona evaporation model provides a promising explanation for not only the state transition, but also the observational features of BHXRBS aforementioned. It is, thus, natural to confront the disk corona evaporation model to observations of AGNs to determine its applicability to accreting black holes systems in general.

Investigation of the model reveals that the evaporation feature is independent of the black hole mass. In particular, the coronal temperatures in the inner region of disks around supermassive black holes and in BHXRBS are the same. Furthermore, the radial distribution of the evaporation rate and the mass flow rate when scaled to the black hole mass for both AGNs and BHXRBS are also independent of the mass. Thus, the model can, in principle, be applied to AGNs (Liu & Meyer-Hofmeister 2001), especially given the analogues between the observational features of AGNs and BHXRBS. In this regard, a spectral state transition for AGNs with a luminosity of a few percent of the Eddington value, the truncation of a thin disk for LLAGNs, the presence of iron lines related with both the disk and the corona, and the occurrence of radio jets associated with the evaporative process in disk coronal flows may be expected.

To investigate the disk evaporation/condensation model for AGNs, we outline the basic physics and assumptions of the theoretical model in §2 and discuss its applicability as an interpretative framework for several AGN properties in §3. The implications of the model and the issues that remain to be addressed due to differences between AGNs and BHXRBS are presented in §4.

2. Theoretical Model

The concept of the evaporation of matter via a siphon flow from an accretion disk was originally proposed in the pioneering work by Meyer & Meyer-Hofmeister (1994) to explain the enigmatic phenomenon of the UV lag observed in dwarf novae. Here, the evaporation leads to the formation of a hole in the inner region of an accretion disk, resulting in the retardation of the UV radiation during the onset of an outburst. The model was developed in a more detailed form for application to disks surrounding black holes by Meyer et al. (2000a), who demonstrated the possible truncation of an outer optically thick disk and the consequent formation of an inner optically thin ADAF. Liu et al. (2002a) extended the model to take account of the decoupling of ions and electrons and the effect of Compton

scattering in the inner regions of the disk close to the central black hole. Similar conceptual models, but with differences in detail were advanced in a semi-analytical model proposed by Dullemond & Spruit (2005) and in a vertically stratified model developed by Różańska & Czerny (2000a,b). The incorporation of inflow and outflow of mass, energy and angular momentum from and towards neighboring zones was included by Meyer-Hofmeister & Meyer (2003), and the effect of magnetic fields with consequentially reduced conduction efficiency was investigated by Meyer & Meyer-Hofmeister (2002), Meyer-Hofmeister & Meyer (2006), and Qian, Liu, & Wu (2007). More recently, the model has been further developed to include the condensation of coronal gas to an inner disk (Meyer et al. 2007; Liu et al. 2007; Taam et al. 2008). The basic physics and assumptions of the model are described in the following.

2.1. Model assumptions

We investigate stationary accretion to a non-rotating black hole. The accretion takes place via a standard optically thick and geometrically thin disk (Shakura & Sunyaev 1973) enclosed by a hot, accreting corona. Such a corona may form by processes similar to those operating in the surface of the sun, or from a thermal instability in the uppermost layers of the disk (e.g. Shaviv & Wehrse 1986). Both the disk and corona are individually powered by the release of gravitational energy associated with the accretion of matter affected through viscous stresses. The interaction between the corona and the underlying disk results from the vertical conduction of heat by electrons, mass evaporation/condensation and hence enthalpy flow, and inverse Compton scattering of the disk photons by coronal electrons. The disk evaporation/condensation model takes account of both the mass exchange (mass evaporation/condensation) and energy exchange (conduction and enthalpy flux) between the disk and corona. This is in contrast to classical disk corona models where only radiative coupling is considered (e.g. Haardt & Maraschi 1991). Assuming a radial one zone approximation, we investigate the mass flow and energy balance in the corona and calculate the detailed vertical structure and radiation emitted from the corona and disk as functions of the viscosity parameter in the corona, black hole mass, and mass accretion rate.

2.2. General description of evaporation

For the modeling of the accretion process, the interaction between the disk and corona is an important and distinctive process compared to the case for an ADAF or disk alone. The corona is an ADAF-like accretion flow modified by the vertical heat conduction and inverse Compton scattering of disk photons, which play a key role in cooling the electrons as a con-

sequence of the soft photon flux from the underlying disk. The ions in the corona are directly heated by viscous dissipation, partially transferring their energy to the electrons by means of Coulomb collisions. The energy gained by electrons cannot be effectively radiated away and is conducted to the lower, cooler, and denser coronal layers by electron-electron collisions. In the transition layer, the conductive heat flux is radiated away through bremsstrahlung only if the number density in this layer reaches a critical value. If the density is too low to efficiently radiate the energy (lower than the critical value), a certain amount of lower, cooler gas is heated up, whereby the bremsstrahlung cooling rate is raised, until an energy equilibrium is established between the conduction, radiation and heating of the cool gas. The transfer of gas from the disk to the corona, to establish the equilibrium, is called evaporation. It occurs in the low density coronae. If the density is so high that bremsstrahlung is more efficient than the conductive heating, a certain amount of gas is over-cooled and condenses onto the disk until energy equilibrium is reached. This condensation process takes place in the high-density corona. Efficient cooling processes such as strong inverse Compton scattering of the disk photons can also facilitate such condensation.

The gas evaporating into the corona retains angular momentum and differentially rotates around the central object. By frictional stresses, the gas loses angular momentum and drifts inward in such a way that the corona continuously drains gas towards the central object. The coronal accretion flow is re-supplied by continuous evaporation and, therefore, steady flows are established in the disk and corona with the mass exchange between the two flows.

In the disk corona model, we assume that the accreting gas is cold and thus enters the disk rather than a corona as occurs in a binary system where the mass transferred from the donor star is constrained to the orbital plane. That is, we do not consider the possibility that the accreting gas enters the disk as a corona (see discussion in sect.4.2), which may be appropriate for the Galactic Center or for very low luminosity AGNs. Hence, the model is restricted to systems in the low/hard state and not necessarily to the very low quiescent state. Within our approximation, the coronal accretion is supplied by evaporating disk matter at distances remote from the accreting black hole. The mass flow rate through the corona at a given distance is the sum of the mass evaporation from the outer edge of the disk inward to a given distance. Hence the mass flow rate in the corona increases toward the black hole as a result of the radial contribution to the mass evaporation, notwithstanding the possible loss of gas due to disk outflows. Note that it is possible that the mass flow rate contributed by evaporation in the outer region is sufficiently high that evaporation ceases at some radius and condensation takes place in the inner region.

In the following, the equations which include the detailed physical processes described above are given. The model used here is based on Liu et al. (2002a) and includes modi-

fications (Meyer-Hofmeister & Meyer 2003) and updates incorporated in recent years (e.g. Qian, Liu, & Wu 2007; Qiao & Liu 2009).

Equation of state

$$P = \frac{\Re\rho}{2\mu}(T_i + T_e). \quad (1)$$

Equation of continuity

$$\frac{d}{dz}(\rho v_z) = \eta_M \frac{2}{R} \rho v_R - \frac{2z}{R^2 + z^2} \rho v_z. \quad (2)$$

Equation of the z -component of momentum

$$\rho v_z \frac{dv_z}{dz} = -\frac{dP}{dz} - \rho \frac{GMz}{(R^2 + z^2)^{3/2}}. \quad (3)$$

The energy equation of the ions

$$\begin{aligned} & \frac{d}{dz} \left\{ \rho_i v_z \left[\frac{v^2}{2} + \frac{\gamma}{\gamma-1} \frac{P_i}{\rho_i} - \frac{GM}{(R^2+z^2)^{\frac{1}{2}}} \right] \right\} \\ &= \frac{3}{2} \alpha P \Omega - q_{ie} \\ &+ \eta_E \frac{2}{R} \rho_i v_R \left[\frac{v^2}{2} + \frac{\gamma}{\gamma-1} \frac{P_i}{\rho_i} - \frac{GM}{(R^2+z^2)^{\frac{1}{2}}} \right] \\ &- \frac{2z}{R^2+z^2} \left\{ \rho_i v_z \left[\frac{v^2}{2} + \frac{\gamma}{\gamma-1} \frac{P_i}{\rho_i} - \frac{GM}{(R^2+z^2)^{\frac{1}{2}}} \right] \right\}, \end{aligned} \quad (4)$$

where q_{ie} is the energy exchange rate between the electrons and the ions,

$$q_{ie} = \left(\frac{2}{\pi} \right)^{\frac{1}{2}} \frac{3}{2} \frac{m_e}{m_p} \ln \Lambda \sigma_T c n_e n_i (\kappa T_i - \kappa T_e) \frac{1 + T_*^{\frac{1}{2}}}{T_*^{\frac{3}{2}}} \quad (5)$$

with

$$T_* = \frac{\kappa T_e}{m_e c^2} \left(1 + \frac{m_e T_i}{m_p T_e} \right). \quad (6)$$

The energy equation for both the ions and the electrons is

$$\begin{aligned} & \frac{d}{dz} \left\{ \rho v_z \left[\frac{v^2}{2} + \frac{\gamma}{\gamma-1} \frac{P}{\rho} - \frac{GM}{(R^2+z^2)^{1/2}} \right] + F_c \right\} \\ &= \frac{3}{2} \alpha P \Omega - n_e n_i L(T_e) - q_{\text{Comp}} \\ &+ \eta_E \frac{2}{R} \rho v_R \left[\frac{v^2}{2} + \frac{\gamma}{\gamma-1} \frac{P}{\rho} - \frac{GM}{(R^2+z^2)^{1/2}} \right] \\ &- \frac{2z}{R^2+z^2} \left\{ \rho v_z \left[\frac{v^2}{2} + \frac{\gamma}{\gamma-1} \frac{P}{\rho} - \frac{GM}{(R^2+z^2)^{1/2}} \right] + F_c \right\}, \end{aligned} \quad (7)$$

where $n_e n_i L(T_e)$ is the bremsstrahlung cooling rate, of which the radiative cooling function $L(T_e)$ is taken from Raymond et al. (1976). Here, q_{Comp} is the Compton cooling rate,

$$q_{\text{Comp}} = \frac{4\kappa T_e}{m_e c^2} n_e \sigma_T c u, \quad (8)$$

with u the energy density of the soft photon field. The thermal conduction flux, F_c , is given by (Spitzer 1962)

$$F_c = -\kappa_0 T_e^{5/2} \frac{dT_e}{dz} \quad (9)$$

with $\kappa_0 = 10^{-6} \text{erg s}^{-1} \text{cm}^{-1} \text{K}^{-7/2}$ for a fully ionized plasma.

All parameters in the above equations are in cgs units and are defined as follows. Specifically, P, ρ, T_i and T_e are the pressure, density, ion temperature and electron temperature respectively. The vertical and radial speed of the mass flow are denoted by v_z and v_R . In Eq.(1), $\mu = 0.62$ is the mean molecular weight assuming a standard chemical composition ($X = 0.75, Y = 0.25$) for the corona. The number density of the ions, n_i , is assumed equal to that of the electrons, n_e , for convenience, which is strictly true only for a pure hydrogen plasma. In the continuity and energy equations, the terms starting with $2z/(R^2 + z^2)$ derive from the gradual expansion of the vertical flow channel with height as the geometry changes from cylindrical to spherical, and η_M is the mass advection modification term and η_E is the energy modification term. These terms parameterize the difference between lateral inflows and outflows. We take $\eta_M = 1$ for the case without consideration of the effect of mass inflow from the outer neighboring zone of the corona, and $\eta_E = \eta_M + 0.5$ is a modification to the previous energy equations (for details see Meyer-Hofmeister & Meyer 2003). The other quantities are as follows: G is the gravitational constant, M the mass of the accreting black hole, m_p and m_e are respectively the mass of the proton and the electron, κ is the Boltzmann constant, c the speed of light, a the radiation constant, σ Stefan-Boltzmann constant, σ_T the Thomson scattering cross section, $\gamma = 5/3$ is the ratio of specific heats, and $\ln \Lambda = 20$ is the Coulomb logarithm.

The five differential equations, Eqs.(2), (3), (4), (7), and (9), which contain five variables $P(z), T_i(z), T_e(z), F_c(z)$, and $\dot{m}(z) (\equiv \rho(z)v_z)$, can be solved with five boundary conditions. In particular, at the lower boundary of the interface between the disk and corona, the conductive flux is exactly radiated away and there is no downward heat flux. The temperature of the gas should be the effective temperature of the accretion disk. Previous investigations (Liu, Meyer, & Meyer-Hofmeister 1995) show that the coronal temperature increases from the effective temperature to $10^{6.5} \text{K}$ in a very thin layer and that the conductive flux can be expressed as a function of pressure at this temperature. Thus, the lower boundary conditions can be reasonably approximated (Meyer et al. 2000a) as

$$T_i = T_e = 10^{6.5} K, \text{ and } F_c = -2.73 \times 10^6 P \text{ at } z = z_0. \quad (10)$$

At infinity, there is no artificial confinement and hence no pressure. This requires a sonic transition at some height $z = z_1$. As there is no heat flux from/to infinity we constrain the upper boundary as,

$$F_c = 0 \text{ and } v_z^2 = V_s^2 \equiv P/\rho = \frac{\Re}{2\mu}(T_i + T_e) \text{ at } z = z_1. \quad (11)$$

With the above boundary conditions, we assume a set of trial lower boundary values for P and \dot{m} to start the integration along z . Only when the trial values for P and \dot{m} fulfill the upper boundary conditions can the presumed P and \dot{m} be taken as true solutions of the differential equations.

2.3. Caveats

In order to reveal the basic properties of disk corona in AGNs, we make some simplifications and approximations. Specifically, we assume an α prescription for the viscosity. In reality, the disk corona structure depends on the magnitude and functional form of the viscosity. This is likely due to magnetic effects associated with the magnetorotational instability (see Balbus & Hawley 1991), though its effectiveness in providing a sufficiently large α remains to be understood (see King, Pringle & Livio 2007). The magnetic field also influences the rate of heating (via non-ideal effects associated with magnetic reconnection) and cooling of the system since non-thermal radiation processes associated with synchrotron radiation and synchrotron self-Compton emission could be operating. In addition, the field can reduce the effectiveness of the vertical heat conduction. Thus, the field likely plays an important role in determining the structure of the disk corona and emission features if sufficiently strong. The irradiation from the hot corona could also become important in heating the disk if the coronal radiation is very strong compared to the disk. This may occur at accretion rates when the disk starts to be truncated. Its affect is relatively unimportant at very low accretion rates when the disk can be truncated and most of the coronal radiation can escape. In addition, at very high accretion rates, the corona irradiation is not as important as the disk radiation itself although there are indications that the coronal emission can be comparable to the optical emission in some AGNs. The irradiation can also be important if most of the accretion energy is released in the corona (e.g. Haardt & Maraschi 1991; Nakamura & Osaki 1993; Kawaguchi et al. 2001), but the nature of the mechanism resulting in such an hypothesis remains unknown. Therefore, we do not consider the effect of irradiation from the inner corona in our level of approximation. With these qualifications, we study the vertical structure in detail, determining the radial flow owing to the vertically distinct flows in the context of the lower cool disk and upper hot coronal flows.

3. Evaporation Model as Applied to AGNs

Given the mass of a black hole, $M = 10^8 M_\odot$, and viscosity parameter, $\alpha = 0.3$, we perform numerical calculations to obtain the vertical structure of the corona for a range of radii. In these models, the mass evaporation/condensation rate is determined by $\dot{m}_{z0} = \rho v_{z0}$. For simplicity, we neglect the possible mass inflow from an outer neighbor since the evaporation in the outer neighbor region is less efficient than the local evaporation. As there is no other mass supply to the corona, the mass flow rate in the corona corresponds to the sum of the evaporation rate, $\dot{M}_{\text{evap}} = 2\pi R^2 \dot{m}_{z0}$, from all radii in the disk. This rate directly determines the relative strength of the corona to the disk as measured by the mass inflow rate and hence the emergent spectrum. In Figure 1, the variation of the mass evaporation rate with the distance is illustrated. Note that the evaporation rate shown in the figure is scaled to the Eddington accretion rate, $\dot{M}_{\text{Edd}} = 1.39 \times 10^{18} M/M_\odot \text{ g s}^{-1}$, i.e., $\dot{m}_{\text{evap}} = \dot{M}_{\text{evap}}/\dot{M}_{\text{Edd}}$, and the distance is scaled to the Schwarzschild radius, $R_S = 2GM/c^2$, $r = R/R_S$. It can be seen that the evaporation is negligible at regions far from the black hole, increasing with decreasing distance until the rate attains a maximum value, corresponding to $\dot{m} = 0.027$, at a few hundred Schwarzschild radii. For smaller radii, the rate decreases towards the central black hole. The occurrence of a maximal evaporation rate results from the energy balance in the disk corona. In the outer region, the evaporation rate increases toward the central black hole since the released accretion energy increases ($\propto R^{-1}$). However, with an increase of the number density towards the inner region, the radiation becomes more efficient (because the bremsstrahlung energy loss rate is proportional to the square of the number density) and only little gas is heated sufficiently to evaporate. Thus, the evaporation rate reaches a maximum value and decreases in the inner region.

Numerical calculations also show that the distribution of evaporation rate with respect to distance, $\dot{m}_{\text{evap}}(r)$, is independent of the black hole mass, in agreement with our previous finding (Liu et al. 2002a). Therefore, the model has following predictions as applied to AGNs.

3.1. Spectral State transition in AGNs

As described above, the evaporation process diverts the accretion flow from the disk to the corona. Consequently, for accretion rates within the disk lower than the maximal evaporation rate, the disk is completely evaporated within a specific region. This region is filled with coronal gas (see Figure 2), and the accretion takes place in a geometrically thick flow. On the other hand, for accretion rates higher than the maximal evaporation rate, the optically thick disk cannot be significantly depleted at any distance. Thus, the disk

extends to the ISCO with an overlying accreting coronal flow coexisting with the disk, fed by continuous evaporation. The variation of the accretion flow geometry with accretion rate is illustrated in the right panel of Figure 2.

Such an evaporation feature has been successfully applied to interpret the spectral states observed in BHXRBs, which is believed to be caused by the different accretion modes. That is, for luminosities greater than the critical luminosity, the accretion is dominated by the mass flow in the disk with the radiative spectrum described by a multi-color blackbody. The system is in the so-called soft state. In contrast, for luminosities lower than the critical value, the accretion is dominated by the corona/ADAF, resulting in a hard state spectrum. Therefore, the evaporation model predicts a spectral transition from an ADAF to a disk-dominated accretion flow at a critical luminosity corresponding to the maximal evaporation rate. The prediction for AGNs is similar to BHXRBs despite the vast difference in the mass of the black hole because the evaporation feature is independent of the black hole mass.

The value of the maximal evaporation rate is known to depend on the accretion history. In a low/hard state, the radiation from the truncated disk is much less than that from the ADAF/corona, and Compton cooling in the corona due the disk photons can be neglected. Thus, the transition from a low/hard state to a high/soft state can be appropriately described by the solid curve in the left panel of Figure 3. That is, the transition takes place at a luminosity of $0.027L_{Edd}$ assuming a standard viscosity, $\alpha = 0.3$. However, the transition from the soft to hard states takes place at a relatively low accretion rate in comparison to the transition from the hard to soft state. This is because the inverse Compton scattering of the disk photons from the ISCO region during the soft state serves as an additional cooling agent for the coronal gas, which leads to a diminished evaporation rate. In this case, Compton cooling must be included in the energy equation (7). The radiation flux, $F_r = cu$, from the central region as seen by the corona at a distance R is given by

$$F_r = \frac{L}{4\pi R^2} \frac{2z}{(R^2 + z^2)^{1/2}}, \quad (12)$$

where L is the luminosity from the central source, which is related to the central accretion rate by assuming an energy conversion efficiency of 0.1, $L = 0.1\dot{M}c^2$.

Eq.(12) reveals that the coronal structure and evaporation rate now depend on the accretion rate. Based on calculations, it was found that for accretion rates near the values corresponding to the hard-to-soft transition rate the maximal evaporation rate is less than the accretion rate. Hence, the disk cannot be truncated at this accretion rate level. However, the evaporation rate increases with decreasing accretion rates (i.e., decreasing soft photon flux) and once the accretion rate decreases to $\dot{m} \approx 0.005$, the maximal evaporation rate equals the accretion rate. This signifies the onset of disk truncation by evaporation at $\dot{m} \approx 0.005$ during

the decay of the outburst, as shown by the dashed line in the left panel of Figure 3. For even lower accretion rates, the disk is truncated and the accretion flow is dominated by the ADAF/corona. Therefore, the soft-to-hard state transition takes place at $\dot{m} \approx 0.005$, which is ~ 5 times lower than the accretion rate for the hard-to-soft state transition. This provides a natural explanation for the so-called luminosity hysteresis observed in BHXRBs (Meyer-Hofmeister et al. 2005; Liu et al. 2005). In AGNs, the different transition luminosities in the soft-to-hard and hard-to-soft states imply that objects with luminosities in the range $0.005 < L/L_{\text{Edd}} < 0.027$ can be in either the soft spectral state or hard spectral state. Specifically, if objects are in the rising phase, their spectra are hard; if they are in the decaying phase, their spectra are soft.

This range in luminosity provides a framework by which objects showing a soft spectrum (big blue bump and steep X-ray spectrum) can be observed at luminosity levels which are comparable to objects showing a hard spectrum (without a big blue bump and with a flat X-ray spectrum). Since the accretion timescale is long compared to the observation timescale, the limited observations do not distinguish whether an object is in the rising or decaying phase. The model provides a potential method to determine the phase of variation if the luminosity level lies between the transition luminosities. That is, for an object with $0.005 < L/L_{\text{Edd}} < 0.027$ exhibiting a hard spectrum, it is either a persistent source or, if transient, in the rising phase and a transition to a soft state is expected to follow, while a soft spectrum indicates the object is in the decaying phase with a subsequent transition to a hard state expected. The overlap in the Eddington ratio for the soft and hard spectral states predicted by our model could also lead to a misclassification of AGN sub-types.

To summarize, the evaporation model predicts that objects characterized by luminosities less than $\sim 0.005L_{\text{Edd}}$ are in the low/hard states, whereas those objects with luminosities greater than $\sim 0.027L_{\text{Edd}}$ are in the high/soft state. Within the luminosity range $0.005L_{\text{Edd}}$ and $0.027L_{\text{Edd}}$ the objects can be either in the high/soft state or in the low/hard state, depending on their secular variability. Objects in this luminosity range may undergo variation with possible transition to another state.

Observationally, spectral state transitions are difficult to detect, although extensive studies on nearby galaxies (for a review see Ho 2008; Ho 2009) suggest that the galactic nuclei evolve through distinct states in response to changes in the mass accretion rate. In the sample of Ho (2009), objects are largely systems in the low or quiescent state, for which the Eddington ratios and corresponding accretion rates are all below the critical accretion rate predicted by the disk evaporation model.

Finally, we point out that the quantitative predictions of the evaporation model depend on the viscosity parameter, α , chosen to be 0.3. Larger values of α result in higher

evaporation rates and smaller transition radii. Here, the greater viscous heating leads to greater conduction of heat to the disk surface, facilitating evaporation. As a result, the critical luminosities of the soft-to-hard and the hard-to-soft transition also depend on α . For example, the critical luminosities of the hard-to-soft transition range from 1% to 10% of the Eddington luminosity for $0.2 < \alpha < 0.6$ (Qiao & Liu 2009).

Observational estimates for α in binary star systems have been summarized in King, Pringle, & Livio (2007), showing viscosity parameters to be $0.2 \lesssim \alpha \lesssim 0.6$ (values are converted according to the definition $\nu = 2/3\alpha c_s H$ as used here). However such estimates for AGN are severely lacking. In a few cases, constraints have been established. For example, the investigation of optical variability in AGNs (Starling et al. 2004) suggests a very low viscosity parameter, $0.01 \lesssim \alpha \lesssim 0.03$, if the optical emission is generated in a standard, fully ionized thin disk and the variability time scale is attributed to the disk thermal timescale. Nevertheless, these values are noted to be lower limits because shorter time-scales may have been missed (Starling et al. 2004).

3.2. The size of broad line region

Broad lines are a distinguishing feature of type 1 AGNs. Hints concerning their origin and nature have been inferred from the empirical relation between the size of broad line region (BLR) and its bolometric luminosity, $R_{\text{BLR}} \propto L_{\text{bol}}^{1/2}$, commonly believed to be a consequence of photoionization of the BLR gas by continuum radiation emitted from the accreting central regions. The formation of the BLR has been connected with radiatively driven winds launched from the disk surface (Murray & Chiang 1997). If the BLR is, indeed, associated with the disk through winds, truncation of the disk leads to truncation of the BLR.

An essential feature of the disk evaporation model is the truncation of a disk for accretion rates below a critical value. For decreasing rates below this value, the inner radius of the disk increases. This property predicts the existence of a region where broad lines would be excluded in a plane described by the line width and Eddington ratio. The variation of the truncation radius with respect to Eddington ratio from the numerical calculations is illustrated in Fig.4, where it is assumed that $L_{\text{bol}}/L_{\text{Edd}} = \dot{m}$ for simplicity. If a lower efficiency of energy conversion is applied to lower accretion rates, the curve is flatter at lower Eddington ratios. The model predicts that the broad line region lies to the above/right of the truncation curve. The region lying below the curve corresponds to the region of exclusion.

Three truncation curves are plotted in Fig.4, showing the dependence of the region of exclusion on the viscosity and evolutionary stage of an AGN. The solid ($\alpha = 0.3$) and dotted

($\alpha = 0.2$) lines delineate this region for objects during the rise in outburst. The difference between these two curves indicates the sensitivity for the location of the excluded region boundary to the viscosity parameter. The dash-dotted curve represents the case for objects during decay from a soft state for a standard viscosity parameter $\alpha = 0.3$, which reveals the dependence of the exclusion region boundary on the evolutionary history. Therefore, the model predicts a region of exclusion for the occurrence of broad lines under the dash-dotted curve, if a standard viscous parameter is adopted, irrespective of the temporal variation of the AGN. In the regime between the solid and dash-dotted curve, broad lines can be present only for objects decaying from a soft state.

To compare with observations, we take the full sample of 35 reverberation-mapped AGNs (Kaspi et al. 2000; 2005; Peterson et al. 2004) after optical correction of the host-galaxy star light (Bentz et al. 2006; 2009). The size of BLR, in units of Schwarzschild radius, versus the Eddington ratio is plotted in Figure 4. The empirical relations of the BLR size with respect to Eddington ratio are also plotted in the figure for different black hole masses. It can be seen that most of the data fall into the region between the empirical lines for $M = 10^7 M_\odot$ and $M = 10^9 M_\odot$ since this is the main range of black hole masses of the sample. However, at low luminosities ($L_{\text{bol}}/L_{\text{Edd}} \lesssim 0.01$), the BLR size does not continually decrease along the empirical lines. Therefore, we suggest that the BLR, which is described by the empirical relation, is "truncated" at low Eddington ratios to a distance corresponding to the inner edge of the evaporation-truncated disk. With decreasing Eddington ratios, the disk recedes outwards and hence the inner edge of the BLR increases until the ionization of the supposed BLR is insufficient for the emission of broad lines. The data in this small sample is in approximate agreement with this prediction, though additional data at low luminosities are necessary to confirm it.

A detailed investigation of the connection between the BLR and disk truncation was also carried out in an earlier work by Czerny et al (2004) for a very large sample of AGNs. It was found that the strong ADAF principle, based on the hypothesis that accretion is via an ADAF whenever an ADAF can exist, better describes the observational data than the disk evaporation model. We point out that a very small value of the viscosity parameter (0.02 for evaporation model and 0.04 for ADAF model) was required in that study, which is not necessary in the present study. Upon comparison of the two versions of evaporation model, we find that our detailed numerical calculations of the vertical structure of disk corona exhibit a dependence of the truncation radius on the viscosity and magnetic fields than from the approximation-based generalized model (Różańska & Czerny 2000b). In particular, a large deviation occurs at Eddington ratio close to the critical transition value. Specifically, our model reveals that a small change in α results in a large change in the critical Eddington ratio characterizing disk truncation ($\dot{m}_{\text{crit}} \propto \alpha^{2.34}$), as illustrated in Figure 4 for α varying

from 0.2 to 0.3. This sensitivity allows for the possibility of an inner disk and hence very broad lines at low Eddington ratios by decreasing α only slightly. In contrast, the weak dependence of truncation radius on α as used in Czerny et al. (2004) leads to a very small value for α in order that broad lines be present at low Eddington ratios. With our detailed numerical model, we expect that the observational sample adopted by Czerny et al. (2004) can also be explained provided that $\alpha \sim 0.1$. This implies that it is unnecessary to assume very small α when the detailed disk evaporation model is used to explain the broad line emissions. In this sense, the disk evaporation model is not as restrictive as compared to models based on the strong ADAF principle.

We note that the theoretical curves are nearly parallel at low Eddington ratios and that the truncation radii are not as sensitive to α in this regime as compared to Eddington ratios of ~ 0.01 . For a normal viscosity value and assuming an appropriate ionization, Fig.4 shows that the broad line region can be present at Eddington ratios as low as ~ 0.001 . However, the size of BLR is not as small as described by the empirical law since the evaporation truncates the inner part or all of the BLR at low Eddington ratios. Therefore, the disk evaporation model predicts two regimes in which the broad lines are "narrower": one corresponding to very low L/L_{Edd} where the disk is truncated at large distances associated with a large broad line region (i.e. LLAGNs, for a review see Ho 2008); the other is at very high L/L_{Edd} where a full disk is present, but its partially ionized region is at large distances (such as the NLS1s). Caution is necessary because there exist uncertainties in the observational data and the adopted parameters in spectral fitting, both of which could lead to large error bars in the derived accretion rate and truncation radius.

3.3. The lower limit to the luminosity for the existence of a broad line region and the occurrence of "True Seyfert 2" Galaxies

For very low accretion rates the disk is truncated at large distances by evaporation. For instance, the disk is truncated at $6600R_S$ at $\dot{m} = 0.001$ (in the case of standard viscosity $\alpha = 0.3$ and no magnetic fields). If regions at such large distances can still emit broad lines, the emission line would be quite narrow. The FWHM of emission lines, as estimated by the Keplerian velocity with a correction factor $2/\sqrt{3}$ (which accounts for velocities in three dimensions and the full width corresponding to twice the velocity dispersion), is given by

$$FWHM = \frac{2}{\sqrt{3}} \sqrt{\frac{GM}{R_{\text{BLR}}}} = \sqrt{\frac{2c^2}{3R_{\text{BLR}}/R_S}} \quad (13)$$

Thus, at $R_{\text{BLR}} = 6600R_S$, the FWHM of emission line is $\sim 3000 \text{ km s}^{-1}$. If we take 2000 km s^{-1} as the critical linewidth between broad line AGNs and narrow line Seyfert 1 galaxies,

we obtain an inner radius of the BLR as $15,000R_s$. To truncate the disk to this distance, the accretion rate should be 4×10^{-4} in units of the Eddington rate as derived from the disk evaporation model. At even lower accretion rates, the disk is truncated at a larger radius and hence the BLR would no longer be recognizable. Therefore, the disk corona evaporation model predicts that the lower limit to the luminosity for the inference of a BLR is $\sim 0.0004 - 0.001L_{Edd}$.

The lower limit to the luminosity of AGNs characterized by a BLR implies that the orientation based unification model is not applicable to LLAGNs. Instead, objects with Eddington ratios lower than ~ 0.001 may intrinsically lack a BLR rather than simply be obscured by a torus. In other words, the model predicts that there exist so-called “true Seyfert 2” galaxies. This is supported by the observations of Bianchi et al. (2008), who discovered an unobscured Seyfert 2 galaxy, NGC 3147, without a BLR. The Eddington ratio for this object ranges roughly between 8×10^{-5} and 2×10^{-4} . Similar discoveries of naked AGNs, characterized by the absence of a BLR accompanied by strong continuum emission and strong variability in the optical band and/or without significant intrinsic absorption in X-rays, indicate that these sources genuinely lack a BLR (see Hawkins 2004; Gliozzi et al. 2007).

Observations of Seyfert 2 galaxies (Sy2s) also support the existence of “true Seyfert 2” galaxies. Of the brightest Sy2s only $\sim 50\%$ exhibit the presence of hidden BLRs in their polarized optical spectra (Tran 2001, 2003; Moran 2006). The luminosities of Seyfert 2 galaxies without a hidden BLR have systematically lower luminosity/Eddington ratios (Lumsden & Alexander 2001; Gu & Huang 2002; Tran 2001, 2003; Moran 2006; Bian & Gu 2007) than Sy2s with hidden BLR (obscured by inclination effects). This implies that “true Seyfert 2s” exist at low luminosities. Quantitative investigations of the non-BLR yield an estimate for the threshold of the Eddington ratio of $10^{-1.37}$ for Sy2s (Bian & Gu 2007) and 10^{-2} for naked AGNs (Gliozzi et al. 2007), both of which are higher than the theoretical prediction. We note, however, that large uncertainties exist in estimating the bolometric luminosity from the optical or X-ray luminosity (e.g., the bolometric luminosity in Bian & Gu (2006) should be 1.5dex lower if based on the method used in Gliozzi et al. (2007)), and uncertainties are present in the determination of the black hole mass, both contributing to apparent deviations from the theoretical prediction.

4. Discussion and Remaining Issues

We have shown that a model developed for BHXRBs based on a disk-corona interaction provides a promising interpretative framework for explaining the characteristic observational

features of AGNs. The evaporation of gas leads to truncation of the disk for accretion rates less than a maximal evaporation rate. This characteristic naturally accounts for the distinct states of AGN, viz., a soft spectrum with big blue bump at high luminosities and a hard spectrum at low luminosities. Due to the existence of differing critical mass flow rates describing spectral transitions from the hard state to the soft state and the soft state to the hard state, AGNs characterized by the same Eddington ratio within the critical luminosity interval can be in either state.

Associating the characteristic scale of the broad line region, R_{BLR} , with the disk truncation radius for LLAGNs, the model predicts that the region excluding the presence of broad lines increases with decreasing luminosity for luminosities less than about $0.005 - 0.027L_{Edd}$ for an α viscosity parameter of 0.3. Hence, R_{BLR} departs from the relation $R_{BLR} \propto L^{1/2}$ at these luminosity levels. As a consequence, broad emission lines are only expected for AGNs characterized by mass accretion rates above a given value, if the broad line region is associated with an optically thick accretion disk. Thus, true Seyfert 2 galaxies are expected at sufficiently low luminosities.

As an additional consequence of the disk truncation, a thermal red bump is expected to be present at low Eddington ratios. This expectation is in qualitative agreement with the presence of the so called “big red bump” in LLAGNs (see Ho 1999; 2008). A detailed study on the disk truncation and a comparison with the observational properties of the big red bump is reserved for a future paper.

Although the model’s basic features provide theoretical support for the hypothesis that the accretion process for supermassive black holes in AGNs is similar to the process for stellar mass black holes in BHXRBs, several observational differences exist between these two types of systems. In the following, we discuss these differences and their possible implications for the model.

4.1. Strong coronal flow in AGNs

As the evaporation is saturated to the maximal rate at high accretion rates (Eddington ratios), the accretion flow in the corona cannot increase with the accretion rate after a transition to the soft state. Thus, the accretion flow within the disk (rather than corona) increases with increasing accretion rate. With efficient Compton scattering, the corona component could be even weaker at high accretion rates because the increased disk radiation leads to strong Compton cooling, resulting in the condensation of coronal gas and the reduction of the optical depth in the corona. If we adopt the maximal evaporation rate without Compton

cooling as an upper limit for the corona flow, we obtain an upper limit on the ratio of the mass inflow rates through the corona and disk as

$$\frac{\dot{m}_c}{\dot{m}_d} = \frac{1}{\frac{\dot{m}}{0.027} - 1}, \quad (14)$$

which is also an upper limit to the ratio of the coronal luminosity to the disk luminosity of a source in the high/soft state. For an accretion rate of 0.1 the coronal luminosity is no more than 37% of the disk luminosity and is less than $\sim 3\%$ of the disk luminosity if the system accretes at the Eddington rate. This implies that the spectral index between optical and X-rays, α_{ox} , is very large in luminous AGNs.

However, observations reveal that the X-ray luminosity is comparable with the optical luminosity in some HLAGNs, indicating a strong corona in AGNs (which is similar to the very high state in BHXRBs). To produce such strong X-ray radiation in luminous AGNs, the frictional heating (in the model) is insufficient. To address this conundrum, it has been suggested that a large fraction of accretion energy is transported from the disk to the corona, perhaps due to a magnetic buoyant instability (Liu et al. 2002b; 2003; Cao 2009). Alternatively, the viscosity parameter α in these HLAGNs may be large, supporting a strong corona by means of efficient evaporation. Such a possibility could be a consequence of a larger magnetic Prandtl number in AGNs than in BHXRBs (see Lesur & Longaretti 2007).

4.2. Additional phenomenology

In addition to their apparent strong coronae, AGNs exhibit other observational features which differ from BHXRBs. For example, among the luminous AGNs $\sim 10\%$ are radio-loud QSOs, while jets in BHXRBs appear to quench whenever the objects transit to the high/soft state. This difference may reflect that jets in the high state of BHXRBs are weak or the properties of the magnetic field in the corona, related to the magnetic Prandtl number, are modified (see above) to facilitate jet formation in AGNs.

We also note that soft X-ray excesses are seen in AGNs at high Eddington ratios, but not in BHXRBs. Such excesses appear to be correlated with the presence of the big blue bump. The origin of this excess is unknown, but it has been interpreted in terms of Comptonization in the disk (Kawaguchi et al. 2001) or resulting from a depression of the continuum at X-ray energies in the range 0.7-5 keV by relativistically broadened line transitions of O VII and O VIII (Gierlinski & Done 2004). Its restriction to AGNs remains to be clarified.

The environment of a galactic central region can significantly differ from that for a stellar mass black hole in an X-ray binary system. For example, significant high temperature diffuse

gas has been observed in the Galactic Center, with Sgr A* accreting at very low Eddington ratios, which may also be present in some LLAGNs. Such hot gas would affect the boundary condition on the disk. However, in the case of hot gas joining the evaporating gas in the corona, the corona is not changed significantly. This is a consequence of the fact that the evaporation of the disk is depressed by the directly inflowing gas due to the pressure and energy balance between the disk and the corona. If the density in the corona is too high, the efficient cooling to the corona can even lead to the coronal gas condensing to the disk. Consequently, the corona flow remains similar to the case of evaporation-fed corona. In other words, for a given accretion rate, independent of whether the disk is fed at the outer boundary, or the disk (corona) is partially fed in the form of cold (hot) gas, the accretion flows through the disk and through the corona in regions of a few hundred Schwarzschild radii are expected to be similar.

Finally, the disk instability model may not give rise to large amplitude outbursts (and hence transitions between the low/hard state and the high/soft state) due to the ionization instability in AGNs as in BHXRBs because the α parameter in the cold state may not significantly differ from its value in the hot state (see Menou & Quataert 2001). In this case the variability would be of small amplitude and state transitions would be less dramatic. AGNs would therefore primarily reflect the mass inflow rate from its surrounding region rather than a temporal variation in a non-steady disk. On the other hand, gravitational instabilities may operate in AGNs to give rise to more significant time dependent accretion.

In the future, we plan to carry out additional investigations to quantitatively confront the disk corona model with the detailed observations of AGNs, with comparisons based on a two-temperature corona model (Liu et al. 2002a) incorporating the effect of magnetic fields (Qian et al. 2007) and viscosity (Qiao & Liu 2009). In addition, a study of their differences with respect to BHXRBs will be explored to examine whether they are one of degree rather than of kind.

We are grateful to Friedrich Meyer and Emmi Meyer-Hofmeister for stimulating discussion and comments on the manuscript. We thank Luis Ho for his careful reading of a preliminary version of the manuscript and very helpful suggestions. Bozena Czerny is thanked for the early discussion. Finally, the referee is thanked for the detailed comments which improved the clarity of the paper. Financial support for this work is provided by the National Natural Science Foundation of China (grants 10533050 and 10773028) and by the National Basic Research Program of China-973 Program 2009CB824800. In addition, R.E.T. acknowledges support from the Theoretical Institute for Advanced Research in Astrophysics (TIARA) in the Academia Sinica Institute of Astronomy & Astrophysics.

REFERENCES

- Abramowicz, M. A., Chen, X., Kato, S. Lasota, J-P, & Regev, O, 1995, ApJ, 438, L37
- Agrawal, P. C., Gokhale, G. S., Iyengar, V. S., Kunte, P. K.; Manchanda, R. K., & Sreekantan, B. V. 1972, Ap&SS, 18, 408
- Balbus, S. A., & Hawley, J. F. 1991, ApJ, 376, 214
- Bentz, M.C., Peterson, B.M., Pogge, R.W., Vestergaard, M., & Onken, C.A., 2006, ApJ, 644, 133
- Bentz, M.C., Peterson, B.M., Netzer, H. et al. 2009, ApJ, 697, 160
- Bian, W., & Gu, Q. 2007, ApJ, 657, 159
- Bianchi, S., Corral, A., Panessa, F., Barcons, X., Matter, G. et al. 2008, MNRAS, 385, 195
- Cao, X. 2009, MNRAS, 394, 207
- Czerny, B., Różańska, A., & Kuraszkiewicz, J. 2004, A&A, 428, 39
- Dullemond, C. P., & Spruit, H. C. 2005, A&A, 434, 415
- Elvis, M., Wilkes, B., McDowell, J.C., Green, R.F., Bechtold, J., et al. 1994, ApJS, 95, 1
- Esin, A.A., McClintock, J.E., & Narayan, R. 1997, ApJ, 489, 865
- Falcke, H., Kording, E., & Markoff, S. 2004, A&A, 414, 895
- Fender, R. P., Belloni, T. M., & Gallo, E. 2004, MNRAS, 355, 1105
- Gierlinski, M., & Done, C 2004, MNRAS, 349, 7
- Gliozzi, M., Sambruna, R. M., & Foschini, L. 2007, ApJ, 662, 878
- Gu, Q., & Huang, J. 2002, ApJ, 579, 205
- Haardt, F., & Maraschi, L., 1991, ApJ, 380, L51
- Hawkins, M. R., S. 2004, A&A, 424, 519
- Ho, L. C. 1999, ApJ, 516, 672
- Ho, L. C. 2008, ARA&A, 46, 475
- Ho, L. C. 2009, ApJ, in press

- Honma, F. 1996, PASJ, 48, 77
- Ichimaru, S. 1977, ApJ, 214, 840
- Kaspi, S., Smith, P.S., Netzer, H., Maoz, D., Jannuzi, B. T., & Givon, U. 2000, ApJ, 533, 631
- Kaspi, S., Maoz, D., Netzer, H., & Peterson, B.M. 2005, ApJ, 629, 61
- Kawaguchi, T., Shimura, & Minehige, S. 2001, ApJ, 546, 966
- King, A. R., Pringle, J.E., & Livio, M. 2007, MNRAS, 376, 1740
- Lesur, G., & Langaretti, P-Y. 2007, MNRAS, 378, 1471
- Liang E. P. T., Price R. H., 1977, ApJ, 218, 247
- Liu, B. F., Yuan, W., Meyer, F., Meyer-Hofmeister, E., & Xie, G. Z. 1999, ApJ, 527, L17
- Liu, B. F., & Meyer-Hofmeister, E. 2001, A&A, 372, 386
- Liu, B. F., Mineshige, S., Meyer, F., Meyer-Hofmeister, E., & Kawaguchi, T. 2002a, ApJ, 575, 117
- Liu, B. F., Mineshige S., Shibata K., 2002b, ApJ, 572, L173
- Liu, B. F., Mineshige S., Ohsuga K., 2003, ApJ, 587, 571
- Liu, B. F., Meyer, F., & Meyer-Hofmeister, E. 2005, A&A, 442, 555
- Liu, B. F., Meyer, F., & Meyer-Hofmeister, E. 2006, A&A, 454, L9
- Liu, B. F., Taam, R.E., Meyer-Hofmeister, E. & Meyer, F. 2007, ApJ, 671, 695
- Liu, F. K., Meyer, F., & Meyer-Hofmeister, E. 1995, A&A, 300, 823
- Lu, Ju-Fu, Lin, Yi-Qing, & Gu, Wei-Min 2004, ApJ, 602, L37
- Lumsden, S. L., & Alexander, D. M. 2001, MNRAS, 328, L32
- Maccarone, T. J. 2003 A&A, 409, 697
- Manmoto, T., & Kato, S. 2000, ApJ, 538, 295
- Menou, K., & Quataert, E. 2001, ApJ, 552, 204
- Merloni, A., Heinz, S., & di Matteo, T. 2003, MNRAS, 345, 1057

- Meyer, F., & Meyer-Hofmeister, E. 1994, *A&A*, 288, 175
- Meyer, F., Liu, B.F., & Meyer-Hofmeister, E. 2000a, *A&A*, 361, 175
- Meyer, F., Liu, B.F., & Meyer-Hofmeister, E. 2000b, *A&A*, 354, L67
- Meyer, F. & Meyer-Hofmeister, E. 2002, *A&A*, 392, L5
- Meyer, F., Liu, B. F., & Meyer-Hofmeister, E. 2007, *A&A*, 463, 1
- Meyer-Hofmeister, E., & Meyer, F. 2001, *A&A*, 380, 739
- Meyer-Hofmeister, E. & Meyer, F. 2003, *A&A*, 402, 1013
- Meyer-Hofmeister, E., Liu, B. F., & Meyer, F. 2005, *A&A*, 432, 181
- Meyer-Hofmeister, E. & Meyer, F. 2006, *A&A*, 449, 443
- Moran, E. C., 2007, in the proceeding of *The Central Engine of Active Galactic Nuclei*, ASP Conference Series, Vol. 373, Edited by Luis C. Ho and Jian-Min Wang, p.425
- Murray, N., & Chiang, J. 1997, *ApJ*, 339, 674
- Nakamura, K., & Osaki, Y. 1993, *PASJ*, 45, 775
- Narayan, R., & Yi, I. 1994, *ApJ*, 428, L13
- Narayan, R., & Yi, I. 1995a, *ApJ*, 444, 231
- Narayan, R., & Yi, I. 1995b, *ApJ*, 452, 710
- Narayan, R., Mahadevan, R., & Quataert, E. 1998, in *Theory of Black Hole Accretion Disks*, edited by M. A. Abramowicz, G. Bjornsson, and J. E. Pringle (Cambridge University Press), p.148
- Narayan, R. 2005, *Ap&SS*, 300, 177
- Narayan, R. & McClintock, J. E. 2008, *NewAR*, 51, 733
- Peterson, B. M., Ferrarese, L., Gilbert, K.M., Kaspi, S., Malkan, M.A. et al. 2004, *ApJ*, 613, 682
- Pounds, K. A., Done, C. & Osborne, J.P. 1995, *MNRAS*, 277, L5
- Pounds, K. A., & Vaughan, S. 2000, *New Astron. Rev.*, 44, 411

- Qian, L., Liu, B.F., & Wu, X.-B. 2007, ApJ, 668, 1145
- Qiao, E., & Liu, B. 2009, PASJ, 61, 403
- Raymond, J.C., Cox, D.P., & Smith, B. W. 1976, ApJ, 204, 290
- Różańska, A., & Czerny, B. 2000a, MNRAS, 316, 473
- Różańska, A., & Czerny, B. 2000b, A&A, 360, 1170
- Shakura, N. I., & Sunyaev, R. A. 1973, A&A, 24, 337
- Shapiro, S. L., Lightman, A. P., & Eardley, D. M. 1976, ApJ, 204, 187
- Shaviv, G., & Wehrse, R. 1986, A&A, 159, L5
- Spitzer L., 1962, Physics of Fully Ionized Gases, 2nd edition, Interscience Publ., New York, London
- Spruit, H. C., & Deufel, B. 2002, A&A, 387, 918
- Starling R. L. C., Siemiginowska A., Uttley P., & Soria R., 2004, MNRAS, 347, 67
- Tananbaum, H., Gursky, H., Kellogg, E., Giacconi, R., & Jones, C. 1972, ApJ, 177, L5
- Tran, H. D. 2001, ApJ, 554, L19
- Tran, H. D. 2003, ApJ, 583, 632
- Taam, R. E., Liu, B. F., Meyer, F., & Meyer-Hofmeister, E., 2008, ApJ, 688, 527
- Wang, R, Wu, X.-B. & Kong, M.-Z., 2006, ApJ, 645, 890
- Yuan, F., Quataert, E., & Narayan, R. 2003, ApJ, 598, 301

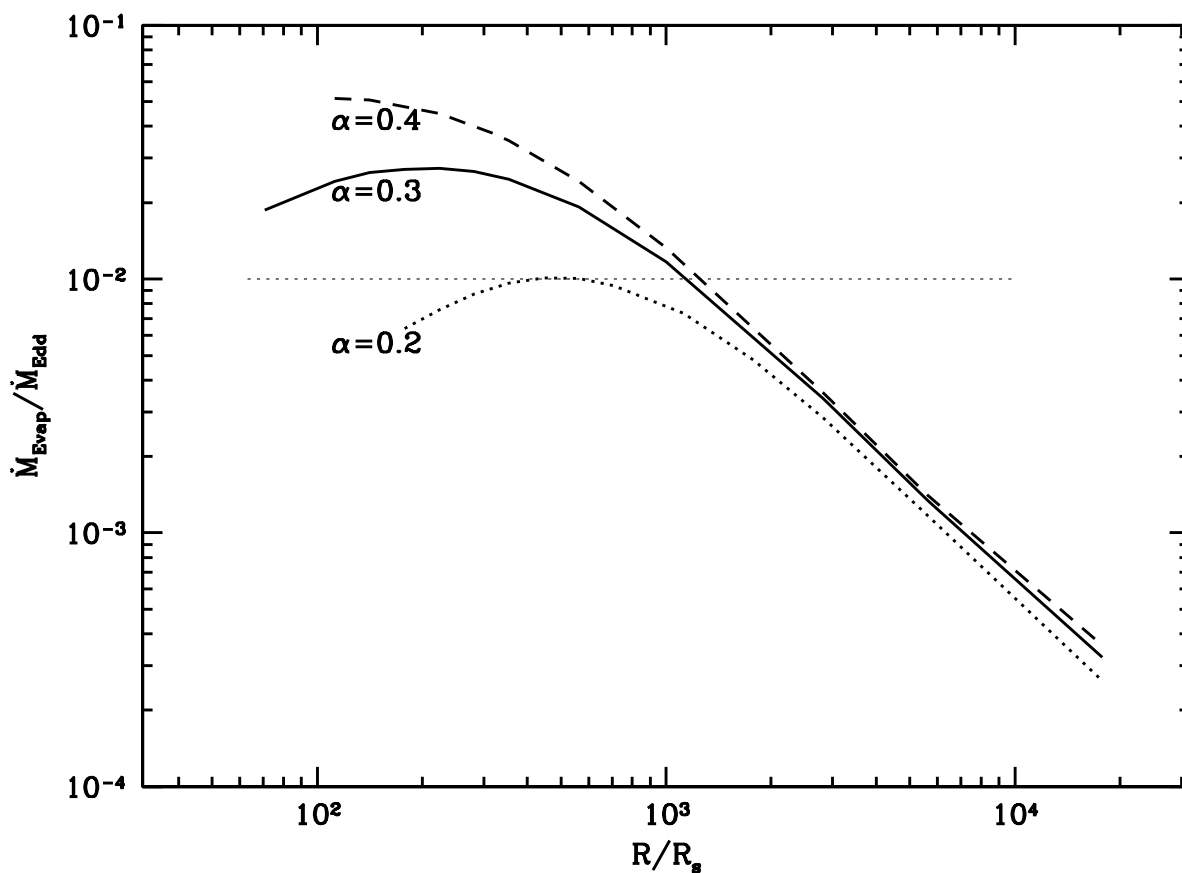


Fig. 1.— The mass evaporation rate as a function of distance. For a standard viscosity parameter, $\alpha = 0.3$, the maximal evaporation rate is $0.027\dot{M}_{\text{Edd}}$, taking place at a distance of $200R_S$ (solid curve). For comparison, the evaporation rate for viscosity parameters, $\alpha = 0.2$ and $\alpha = 0.4$, is illustrated by a dotted curve and dashed curve. Intersections of the thin dashed line with the 3 curves show how the truncation radius varies with the viscosity parameters, as an example of $\dot{m} = 0.01$.

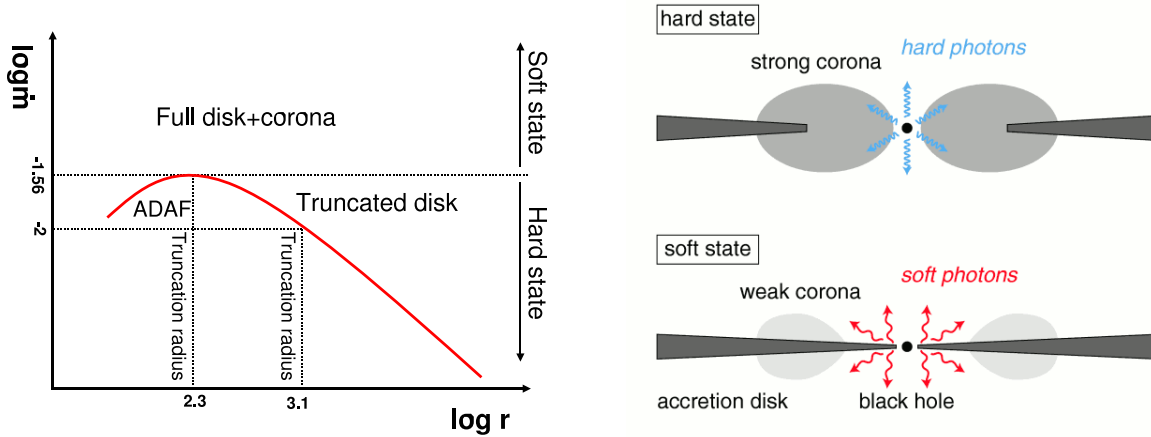


Fig. 2.— A schematic description of disk truncation and the spectral transition illustrating its dependence on the mass accretion rate. The evaporation rate is illustrated as a function of distance in the left panel. At low accretion rates, the disk is truncated by evaporation due to insufficient mass supply at distances determined by the evaporation curve. The accretion flow in the inner region takes place via a corona/ADAF. When the accretion rate exceeds the maximum, which is 0.027 times the Eddington rate in the case for which Compton cooling is unimportant and a standard viscosity parameter ($\alpha = 0.3$), evaporation cannot evacuate any disk region since the mass flow in the disk is greater than the evaporation rate. Thus, the disk extends to the ISCO and dominates the accretion flow. The corona overlying the disk becomes very weak. The figure implies that objects at high accretion rate/luminosity are in a soft spectral state, while below this accretion rate/luminosity, objects are in a hard spectral state with a state transition occurs at an accretion rate corresponding to the maximal evaporation rate. The corresponding accretion geometry is plotted in the right panel.

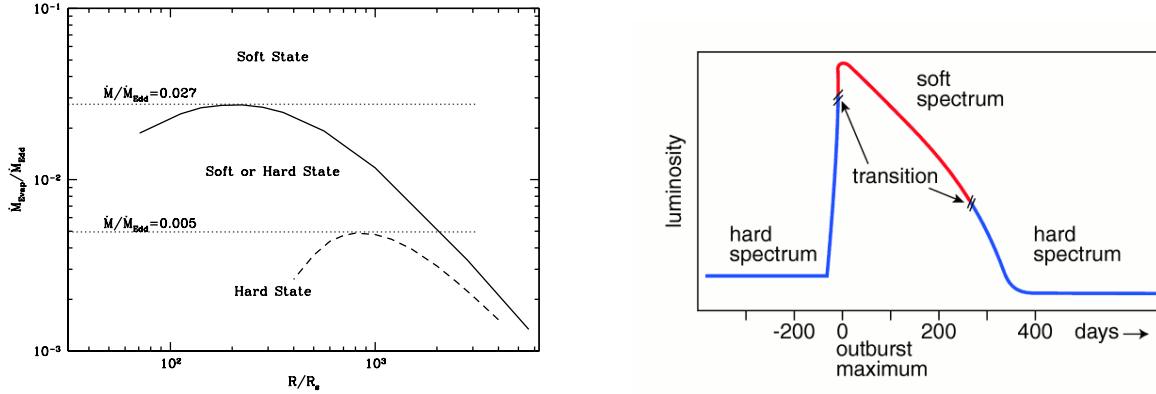


Fig. 3.— Left panel: Model prediction of the spectral states of AGNs and dependence on accretion history. If any inner disk is absent, the maximal evaporation rate is $\dot{m}_{\text{evap,max}} = 0.027$. The state transition takes place at 0.027 times the Eddington rate, as shown in Figure 2. If an inner disk dominates the accretion flow, the evaporation is greatly reduced by Compton cooling of the corona by soft photons from the disk. A transition occurs at an accretion rate of 0.005 times the Eddington value. This implies that the spectral transition from a soft to hard state takes place at $\dot{m} = 0.005$ and from hard to soft at $\dot{m} = 0.027$. Specifically, for an object undergoing an increase in luminosity from a quiescent state, the spectrum is hard until the accretion rate reaches 0.027 times the Eddington value; whilst during the decay phase from a soft state, the transition to a hard state takes place only when the accretion rate decreases to a lower value, $\dot{m} = 0.005$ where the disk is again truncated by evaporation. This description provides an interpretation for the hysteresis observed in BHXRBs. For AGNs, the consequence is, for accretion rates $0.005 \lesssim \dot{m} \lesssim 0.027$, the accretion flow can be dominated either by a disk or by an ADAF. Therefore, the model predicts that objects with an Eddington ratio in the range between 0.005 and 0.027 can be in either the soft state or hard state, depending on its accretion/evolutionary history. Right panel: Schematic light curve of a representative outburst for a typical BHXRB. The transition luminosity from the hard to soft state is higher than that from the soft to hard state, in agreement with the model.

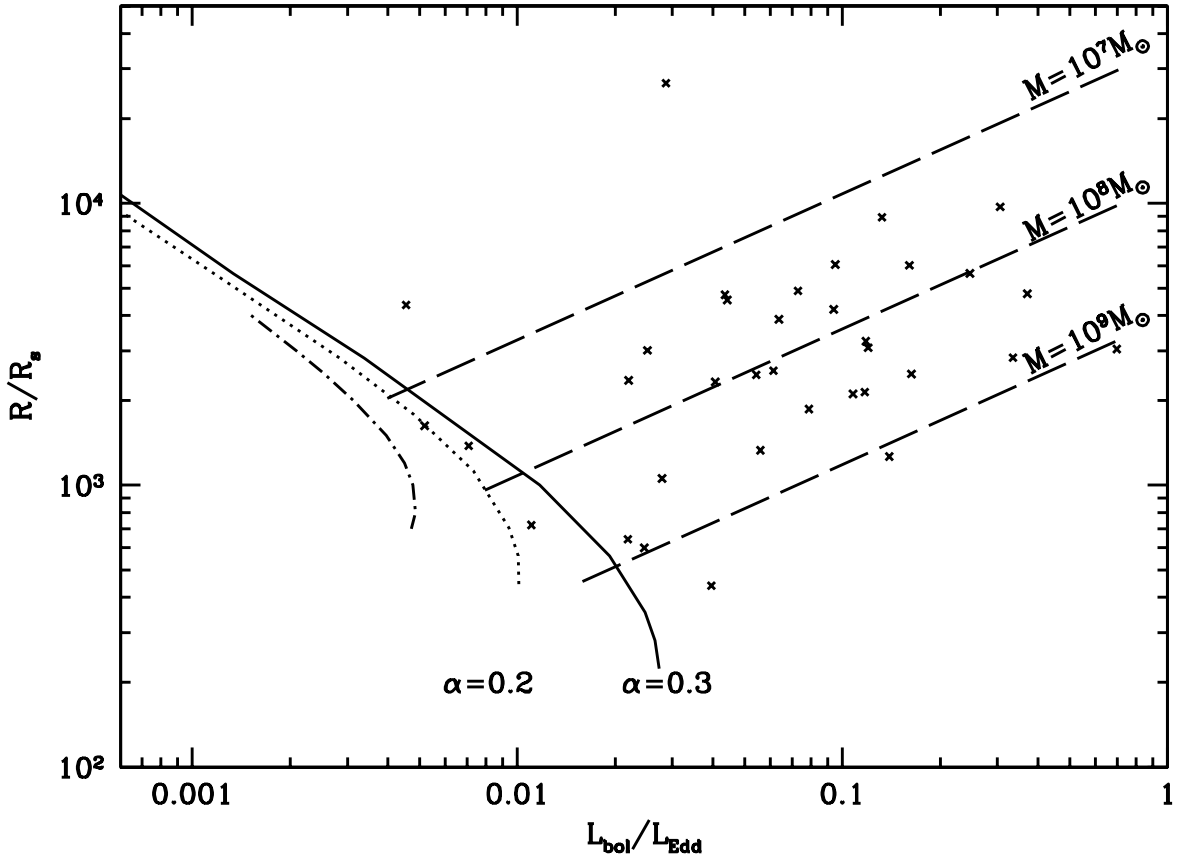


Fig. 4.— The size of BLR vs the Eddington ratio. The data are taken from reverberation mapping of Peterson et al. (2004), Kaspi et al. (2005), and Bentz et al. (2006, 2009). The empirical relations of the size of BLR and Eddington ratio for a black hole mass of $M = 10^7 M_\odot$, $10^8 M_\odot$, and $10^9 M_\odot$ are plotted as long dashed lines. The curves indicate the truncation radius of the disk as a function of Eddington ratio for $\alpha = 0.3$ (solid line) and $\alpha = 0.2$ (dotted line) without Compton cooling and with Compton cooling (dash-dotted line) for the standard viscosity parameter $\alpha = 0.3$. The model predicts an absence of the BLR below the truncation curve because the inner disk is absent in this regime. The broad line can be present in between the solid curve and dash-dotted curve if the object evolves from a soft state. In contrast, it is absent if it evolves from a hard state. The data show that the size of BLR increases with the Eddington ratio along the empirical lines at high luminosities/Eddington ratio, while at very low Eddington ratios, the BLR appears to be “cut out” along the model prediction curve.